MONITORING THE WATER SURFACE AND LEVEL CHANGE IN MUDA AND PEDU DAMS USING MULTI-TEMPORAL SAR DATA

Maizaitoldura Mohd Isa[1], Shahruddin Ahmad[1], Hana Mohamed Jamil[1], Nurul Suliana Ahmad Hazmi[1], Nur Hazwani Izehar[1], Mohamad Faisal Mohamed Yusof[1], Akhmalluddin Mohd Sujai[1] and Shahrul Ikhwan Nasir Shoabani[2]
[1] Malaysian Space Agency (MYSA)
Ministry of Science, Technology, and Innovation (MOSTI) No. 13, Jalan Tun Ismail, 50480 Kuala Lumpur, Malaysia
[2] Muda Agricultural Development Authority
Ministry of Agriculture, and Food Security Ampang Jajar, 05990, Alor Setar, Kedah, Malaysia
maizatuldura@mysa.gov.my; shahruddin@mysa.gov.my; hana@mysa.gov.my; nurulsuliana@mysa.gov.my; hazwani@mysa.gov.my; faisal@mysa.gov.my; akhmalluddin@mysa.gov.my; Shahrul.ikhwan@mada.gov.my

KEYWORDS: Radarsat-2, Sentinel-1, dam, and water level.

ABSTRACT: The efficient management and use of water resources are important for various sectors, including agriculture, hydroelectric power generation, and water supply. Reservoirs play an important role in storing and regulating water supplies, making accurate monitoring of their water levels for effective resource management. Water level monitoring often faces limitations due to factors such as cost, accessibility, and adverse weather conditions. However, with the use of synthetic aperture radar (SAR) satellite images, the water level in the reservoir can be monitored through the use of multi-time SAR images that can accurately detect and monitor reservoir water level changes. The data obtained can be used to generate accurate water level maps, providing a comprehensive view of the reservoir's water distribution. This information can help optimize water allocation strategies, identify potential water leaks or seepage, and manage water supply during droughts or floods. Furthermore, the combination of SAR and the Digital Elevation Model (DEM) can also facilitate the detection of potential issues such as water leakage or seepage, sedimentation, and changes in the shoreline of the reservoir. By identifying these changes in time, resource managers can take proactive steps to address them, ensuring the longevity and sustainability of water resources. Our study area is the Muda and Pedu Dams, located north of Peninsular Malaysia. The Pedu Reservoir receives water from its catchment area (171 square kilometers) as well as inflows from the Muda Reservoir, which is connected through a 6.8 km long tunnel. This dam is very important for rice irrigation in the Mada rice granary area and domestic and commercial water for Kedah and Perlis. This study uses multi-temporal SAR Radarsat-2, and Sentinel-1 data to determine high and low water levels in Muda and Pedu reservoirs during the dry and monsoon seasons. The results show that water area is highly correlated with the water level, while the linear regression between multiple time water area and gauge water level has $r^2 = 0.8$. The extracted water boundary is also overlaid with bathymetry to estimate the volume and generate an accurate water level map, providing a comprehensive view of the distribution of water in the dam. The results of this study show that multi-temporal SAR images can accurately detect and monitor dam water level changes over time.

1. INTRODUCTION

Dams are built to allow the storage of water needed during the dry season and for flood control, recreation, navigation, and hydropower generation (Cochrance et al., 2014). Dam monitoring plays an important role in the detection of unsafe conditions and requires appropriate management actions and countermeasures from an early stage (Tomás et al., 2013). Indeed, early detection of dam instability can form an important component of any dam maintenance plan and can lead to structural stabilization to prevent any early warning from turning into a disaster (Al-Husseinawi et al., 2018). The Muda and Pedu Dams in Malaysia are situated in the northern part of Peninsular Malaysia and serve as freshwater storage for water supply, irrigation, fisheries, and tourism. The dam catchment area is predominantly covered by natural forests, but the reservoir has experienced silting due to logging activities in recent years. Water depletion during the dry season at the Muda and Pedu Dams has been attributed to an increase in sedimentation content within the dam. Therefore, periodic water level monitoring in this area holds immense significance. Satellite images exhibit great potential for water level monitoring and assessment. This study aims to determine high and low water levels in the Muda and Pedu reservoirs during the dry and monsoon seasons, while also establishing a methodology for water level surveillance using multi-temporal Sentinel-1 and Radarsat-2 SAR satellite images. The goal is to enhance dam management effectiveness and develop an operational application system. Synthetic aperture radar (SAR) offers significant advantages over optical systems, providing reliable information for estimating water levels and extracting surface water due to their immunity to cloud cover and illumination independence (Gstaiger et al., 2012). SAR satellite observations offer consistent monitoring and tracking of water level changes in short time intervals between surveys (Shen et al., 2019). The interaction of the radar signal with the surface is characterized by the backscatter-to-return signal proportion (σ^0), which depends on radar design and Earth's surface properties, including terrain, geometry, and roughness, etc. (Lusch, 1999). Calm water surfaces reflect radar signals according to the law of mirrors. As a result, most of the reflected signal does not return to the radar, which is why water bodies on SAR images correspond to very low values of $\sigma 0$. Change detection methods are widely used to identify seasonal flood areas and water bodies. One approach is based on a significant reduction in $\sigma 0$ in watery areas compared to the previous image (O'Hara et al., 2019). Although synthetic aperture radar interferometry (InSAR) observations have been used successfully to study wetland hydrology (Hong et al., 2010 and Wdowinski et al., 2008), this method is suitable for a wide area with a gentle slope where the exposed area depends on the water level. Therefore, the estimation of water levels in lakes and reservoirs with small widths that can be obtained from satellite data remains unknown. A study was successfully introduced to estimate the precise water level in a dam reservoir using accurate boundary extraction and a fine InSAR-based digital elevation model (DEM) (Yoon et al., 2013).

MATERIALS AND METHODOLOGY

2.1 Study Region

Muda and Pedu Dams are in the district of Sik in Kedah, Malaysia. Muda Dam was built in 1969 with the main function as an irrigation water storage reservoir under the Muda Irrigation Scheme to support agricultural development and the rice sufficiency policy. Muda Dam has a large catchment area (984 km^2) but a low storage capacity of 160 million m^3. Therefore, water from the Muda Dam is transferred to the Pedu Dam, which has a higher storage capacity of 1073 million m^3, through the 6.8 km long Saiong Tunnel for water storage and release. This dam started degrading water quality issues due to forest activity. Water quality has an impact on domestic water supply and irrigation for the Muda area in the northern area.

Figure 1. Study Area

2.1 Image Acquisition

Radarsat-2 satellite which was launched by Canada Space Agency (CSA) on December 14, 2007. The spacecraft is owned by MDA (formerly MacDonald Dettwiler and Associates). RADARSAT-2 has one sensor module, and a C-band SAR (Synthetic Aperture Radar) imager. Sentinel-1 consisting of a constellation of two polar-orbiting satellites, operating day and night performing C-band SAR imaging, allowing them to acquire imagery regardless of the weather. The Sentinel-1 satellite platform with GRD product type was downloaded from https://scihub.copernicus.eu/dhus/#/home. Sentinel-1 operates in four (4) modes namely Strip Map (SM), Interferometric Wide swath (IW), Extra-Wide swath (EW) and Wave (WV). Both

Radarsat-2 and Sentinel-1 are active sensors. Active sensors emit energy and measure the reflected or scattered signal, while passive sensors detect the natural radiation or emission from the target or the environment. RADARSAT-2 can operate in single and dual polarisation for beam mode and the nominal resolution is 8 meters. The data obtained is from Sentinel 1, consisting of a constellation of two polar orbiting satellites, operating day and night and performing C-band synthetic aperture radar imaging, allowing them to acquire imagery regardless of the weather.

2.2 Remote Sensing Data

Multi-temporal Synthetic Aperture Radar (SAR) imageries were used in this study to monitor Muda and Pedu water level changes from 2020 to 2023. The water levels in both dams experienced a decrease starting from February 2020 and returning to normal levels by December 2020 due to the dry season. In this study, we used multi-temporal Radarsat-2 and Sentinel-1 images from February 2020 to April 2023 to extract both reservoir water surface areas as shown in Table 1.

Table 1. Summary of the Synthetic Aperture Radar (SAR) data used in this study, which includes a ground-synchronized remote sensing image on the same date.

Type of Sensors	Image Date	Mode	Pixel Spacing (m)
Sentinel-1	29 February 2020	Interferometric Wide Swath (IW)	10 x 10
	15 August 2020		
	14 October 2020		
	13 May 2021		
	13 February 2022		
Radarsat-2	22 March 2022	Wide Extra Fine Quad Pol	9 x 9
	28 March 2023		
	21 April 2023		

2.3 Sigma Nought

Sigma Nought is the backscatter returned to the antenna from a unit area on the ground. It is corrected for the local angle of incidence and is within the range of the ground. Sigma Nought is a common measurement used to evaluate the reflective state of a surface and is independent of geometric effects. Therefore, a digital elevation model (DEM) is required to convert the corresponding input pixel DN value to Sigma Nought. Sigma Nought is often used in the scientific interpretation of SAR images because pixel values are calibrated. SAR images that differ in Sigma Nought values can be compared easily and quickly. In addition, it is used to obtain information about surface scattering mechanisms and surface properties. In the Sigma Nought image, the effect of topography on backscatter is minimized. Backscattering depends on the backscattering properties of the surface and the image appears "flat". It varies with radar wavelength and polarization. Sigma naught in decibels is calculated as follows:

$$\sigma^0 = 10 * log_{10} DN^2 + calibration\ factor \quad (1)$$

For Level-1.1 data, sigma naught is calculated as follows:

$$\sigma^0 = 10 * log_{10}(I^2 + Q^2) + calibration\ factor - 32.0 \quad (2)$$

Where;

I = the imaginary part of the value

Q = the real part of the calibration factor value is obtained from the ALOS metadata

DN refers to a single pixel value

2.4 Filtering

SAR images have high speckle noise; hence, many filters, including Lee, Kuan, Frost, and Gamma MAP have been used to reduce speckle SAR images. Enhance Lee Adaptive Filter, one of the well-known filters, was applied with a 3 x 3 window size.

2.5 Classification

2.5.1 Water Level

Eight (8) Synthetic Aperture Radar (SAR) from 2020 - 2023 were classified into two (2) main water level classes, which are waterbody and land using the Support Vector Machine Classifier (SVM) classifier. All images were SAR imageries.

2.6 Research Flow Chart

The research flowchart is shown in Figure 2.

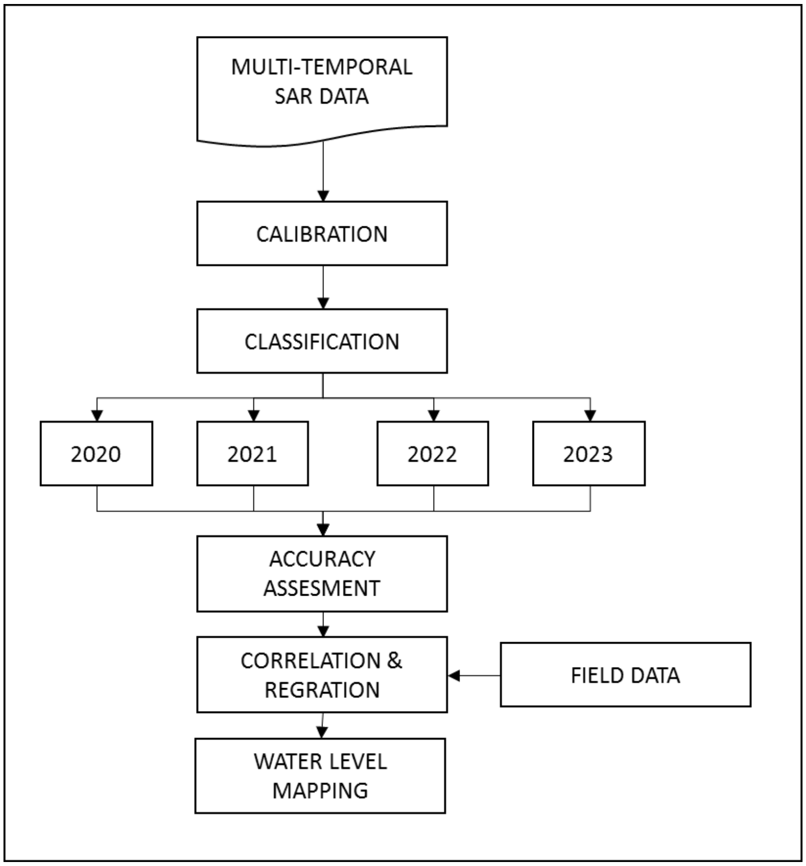

Figure 2**.** Research flowchart.

2.7 The Pearson Correlation Analysis

Correlation analysis is the relationship and direction between two or more variables. This aims to find spectral bands that have a significant relationship with the water level field, which is required to perform regression analysis. Only spectral bands with a significant correlation coefficient (r) can be used as input in the regression analysis. The input pixel values for the empirical model are single band values and band multiplication.

3. RESULTS AND DISCUSSION

3.1 Multi-Temporal Water Level Classification

The classification accuracies for the years 2020, 2021, 2022 and 2023 are 96.9 %, 97.4 %, 97.7% and 96.4 %, respectively. Meanwhile, the kappa statistics values for each year are 0.865, 0.889, 0.835, and 0.831. The classification for this area mostly indicates good classification performance, with Kappa values more than 0.80 (based on the findings from Lillesand et al., 2004; Jensen 2005).

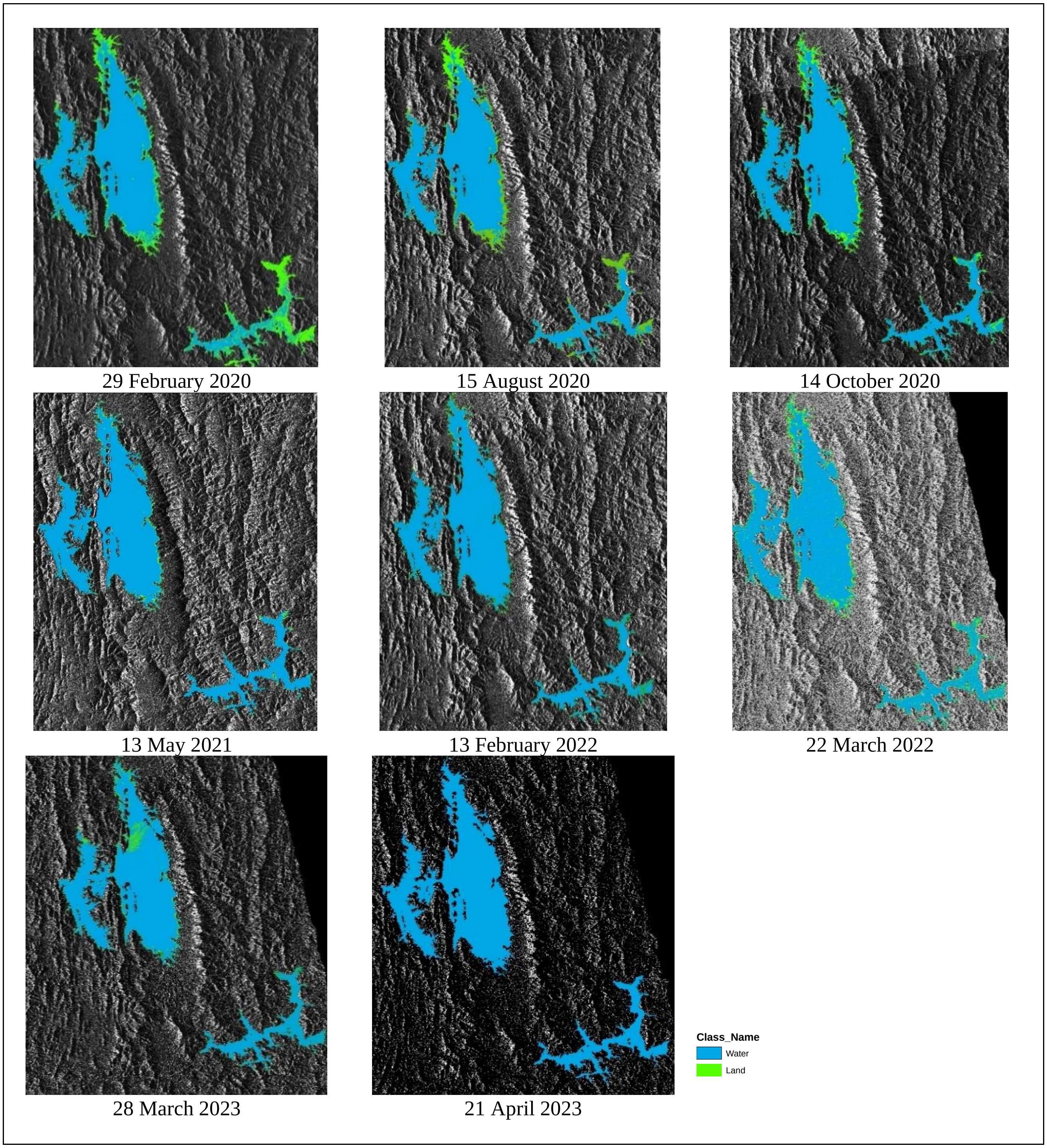

Figure 3. Multi-temporal water level classification

Table 2. Information on imageries used for Pedu and Muda Dam water level classification.

Synthetic Aperture Radar (SAR)	Date	Area (Hectare)	
		PEDU	MUDA
Sentinel-1	29 February 2020	4521.316	820.218
	15 August 2020	4668.879	935.139

	14 October 2020	4900.379	1152.194
	13 May 2021	5157.141	1129.199
	13 February 2022	5301.183	1262.828
Radarsat-2	22 March 2022	5279.824	1163.553
	28 March 2023	5041.716	1147.880
	21 April 2023	5584.988	1375.422

Table 3: 2020 Confusion Matrix

Year: 2020, Overall Accuracy: 96.9 %, Kappa Statistics: 0.865				
LC	**Water**	**Land**	**Total**	**User Accuracy**
Water	10.000	0.000	10.000	1.000
Land	0.000	8.000	10.000	0.800
Producer Accuracy	1.000	0.727	0.000	0.969

Table 4: 2021 Confusion Matrix.

Year: 2021, Overall Accuracy: 97.4 %, Kappa Statistics: 0.889				
LC	**Water**	**Land**	**Total**	**User Accuracy**
Water	10.000	0.000	10.000	1.000
Land	0.000	8.000	10.000	0.800
Producer Accuracy	0.909	0.727	0.000	0.974

Table 5: 2022 Confusion Matrix

Year: 2022, Overall Accuracy: 97.7%, Kappa Statistics: 0.835				
LC	**Water**	**Land**	**Total**	**User Accuracy**
Water	10.000	0.000	10.000	1.000
Land	0.000	9.000	10.000	0.900
Producer Accuracy	1.000	0.700	0.000	0.977

Table 6: 2023 Confusion Matrix

Year: 2023, Overall Accuracy: 96.4 %, Kappa Statistics: 0.831				
LC	**Water**	**Land**	**Total**	**User Accuracy**
Water	10.000	0.000	10.000	1.000
Land	1.000	6.000	10.000	0.600
Producer Accuracy	0.909	0.750	0.000	0.964

3.2 WATER SURFACE AREA ANALYSIS

The water surface area of the Pedu Dam has drastically decreased by 20 percent during the dry season in February 2020 when the daily average temperature is higher. The water surface area back to its maximum capacity in April 2023. Table 7 shows that the water surface area in February 2020 was 4521 ha and increased in August 2020 to 4669 ha and in October 2020 to 4900 ha. In May 2021, the water level increased (5157 ha), followed by February 2022 (5301 ha), and March 2022 (5279 ha). In March 2023, the water level of Pedu Dam experienced a slight decline (5042 ha) and increased back in April 2023 (5585 ha).

Table 7: Pedu Dam Water Surface Area from 2020 to 2023

Month/Year	Feb 2020	Aug 2020	Oct 2020	May 2021	Feb 2022	Mar 2022	Mar 2023	Apr 2023
Water Surface Area (ha)	4521	4669	4900	5157	5301	5279	5042	5585
Percentage	80.96	83.61	87.75	92.35	94.93	94.53	90.29	100

* Total Water Surface Area for Pedu Dam is 5584 ha.

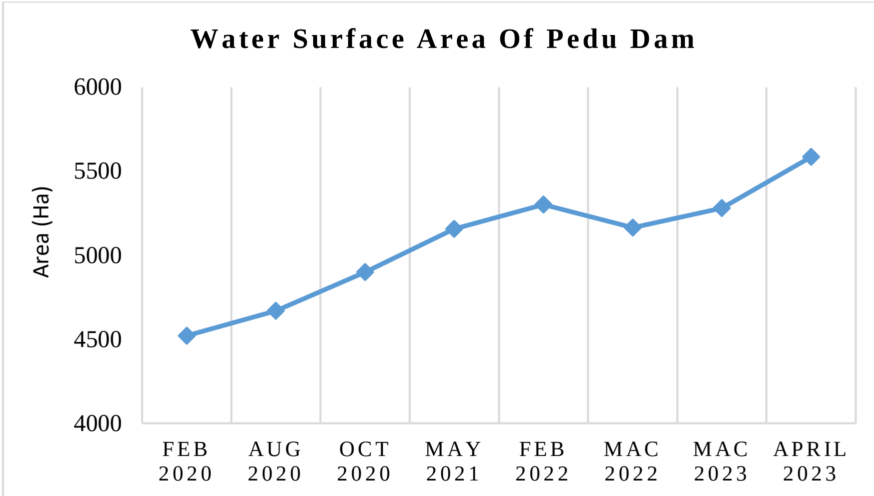

Figure 4: Graph of Pedu Dam Water Surface Area from 2020 to 2023.

The water surface area of the Muda Dam also decreased during the dry season in February 2020. Table 8 shows water level decreased from 820 ha in February 2020 and started to increase from August 2020 (935 ha) and October 2020 (1152 ha). The water surface area continued to decrease in May 2021 (1129 ha), February 2022 (1263 ha) and March 2022 (1164 ha). In March 2023, the water surface area of Pedu Dam experienced a slight decline (1147 ha) and the water level increased back in April 2023 (1375 ha).

Table 8: Muda Dam Water Surface Area from 2020 to 2023.

Month/Year	Feb 2020	Aug 2020	Oct 2020	May 2021	Feb 2022	Mar 2022	Mar 2023	Apr 2023
Water Level Area (ha)	820	935	1152	1129	1263	1164	1147	1375
Percentage	59.6	68	83.8	82.1	91.8	84.65	83.5	100

* Total Area Muda Dam = 1375 ha

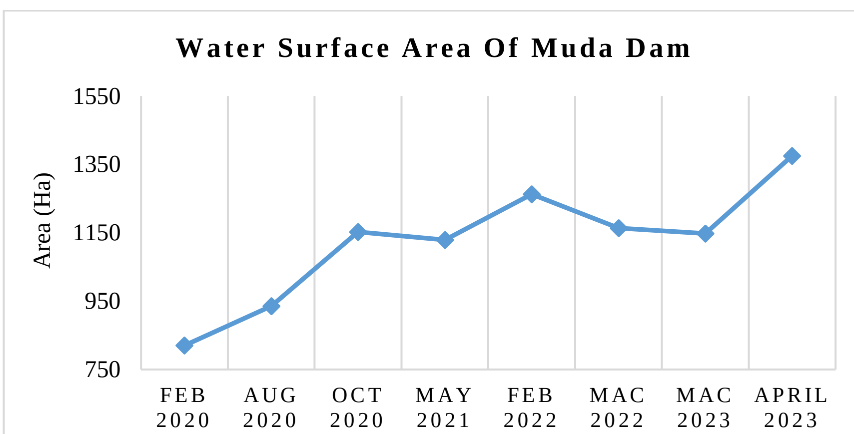

Figure 5: Graph of Muda Dam Water Surface Area from 2020 to 2023.

Table 9 shows the gauge water level reading of Pedu Dam from February 2020 to April 2023. In February 2020 the lowest water level decreased (83.88 m) during dry seasons and slowly increased starting from August 2020 (88.54 m), and October 2020 (92.68 m). In May 2021, the water level increased (95.17 m) but in February 2022 the Pedu Dam water level recorded a slight decline (94.21 m) and in March 2022 (93.88 m). In March 2023 is (94.68 m) and the water level increased back in April 2023 is (96.56 m).

Table 9: Gauge Water Level of Pedu Dam from 2020 to 2023.

Month/Year	Feb 2020	Aug 2020	Oct 2020	May 2021	Feb 2022	Mar 2022	Mar 2023	Apr 2023
Water Level Area (MSL) (m)	83.88	88.54	92.68	95.17	94.21	93.88	94.68	96.56

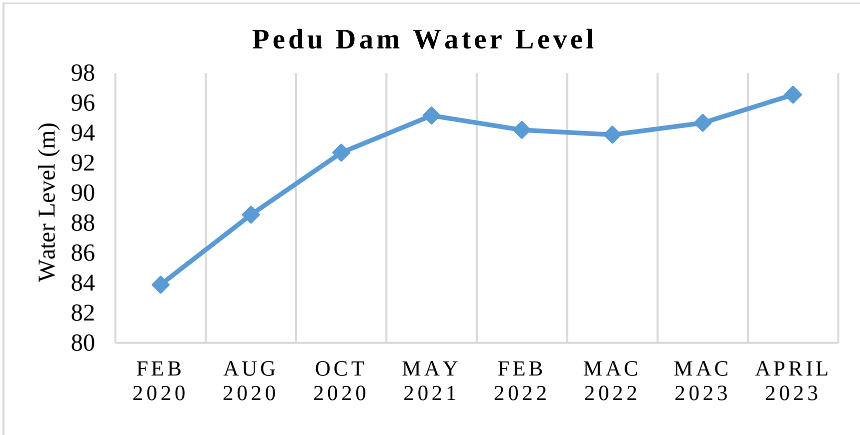

Figure 6: Graph of Pedu Dam Water Level from 2020 to 2023.

The gauge water level of Muda Dam decreased in 2020 as shown in Table 10. Water level in February 2020 shows the lowest gauge reading (84.72 m) and increased back in August 2020 (95.69 m) and October 2020 (98.82 m). In May 2021, the water level increased (98.53 m) but in the year February 2022 Pedu Dam gauge water level light declined (98.31 m), and in March 2022 (98.21 m). In March 2023 is (97.60 m) and the water level increased back in April 2023 is (99.14 m).

Table 10: Gauge Water Level of Muda Dam from 2020 to 2023.

Month/Year	Feb 2020	Aug 2020	Oct 2020	May 2021	Feb 2022	Mar 2022	Mar 2023	Apr 2023
Water Level Area (MSL) (m)	84.72	95.69	98.82	98.53	98.31	98.21	97.60	99.14

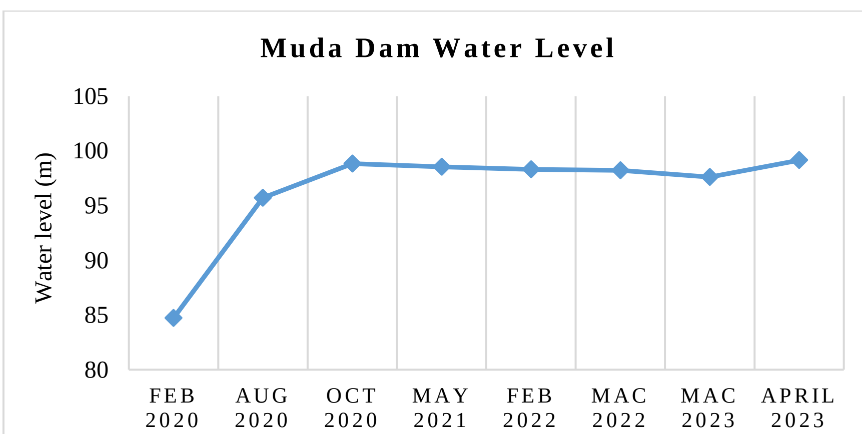

Figure 7: Water Level of Muda Dam from 2020 to 2023.

Figures 8 and 9 show a correlation between water surface area extracted from multi-temporal SAR (Sentinel-1 and Radarsat-2) satellite images with gauge water level data from ground measurement. The results show a strong correlation between satellite and ground-based measurement data, with an r^2 is 0.83 for Pedu Dam and an r^2 of 0.76 for Muda Dam. The linear regression coefficient is determined based on the strength of the correlation coefficient, where 0.31-0.5

represents a weak correlation, 0.51-0.7 means a normal correlation, 0.71-0.90 represents a strong correlation, and 0.91-1.0 represents a strong correlation Yoon, G.W., et al (2013).

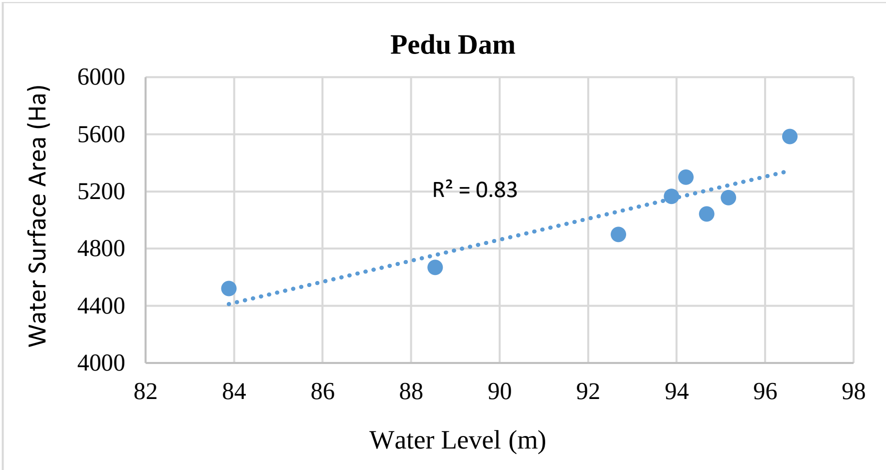

Figure 8. Correlation between gauge measurements of water level and water surface area extracted from multi-temporal SAR at Pedu Dam.

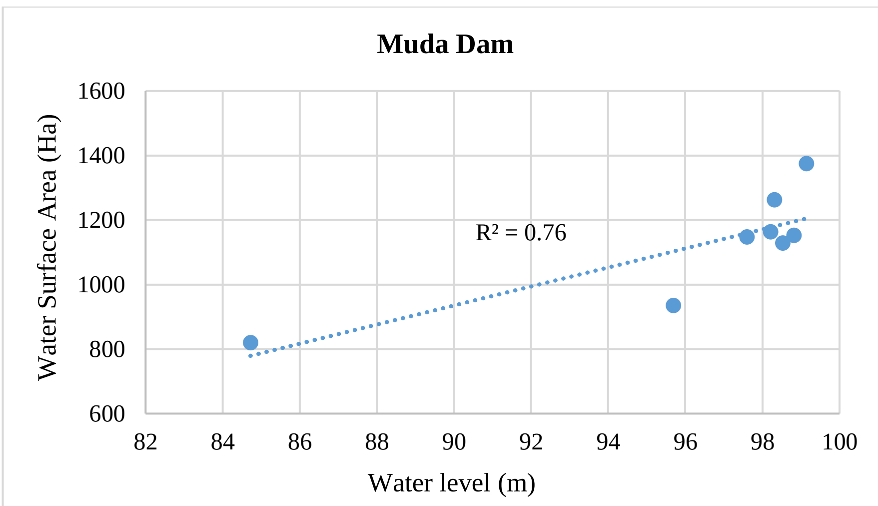

Figure 9. Correlation between gauge measurements of water level and water surface area extracted from multi-temporal SAR at Muda Dam.

4. CONCLUSION

The use of SAR satellite images to extract the surface area of water for the Muda and Pedu dams has been successfully demonstrated. The results of mapping the water level in the Muda and Pedu dam reservoirs using multi-temporal SAR images (Sentinel-1 and Radarsat-2 satellites) show that in 2020, the lowest water surface area in the Pedu and Muda dams during the dry seasons. Prolonged high temperatures in the state of Kedah starting at the beginning of 2020 and until the end of June 2020. This is due to the Northeast Monsoon, which the states in the northern part of the Peninsular experienced drought. The highest temperature recorded in Sik was 35.3 degrees Celsius. This study shows that multi-temporal SAR images are very useful in determining and monitoring water level changes for large coverage areas. In addition, it is an example of a tool for dam monitoring and assists in decision-making at the local level in dam management. The study concluded that SAR images can provide useful information for monitoring and mapping water bodies. More research needs to be done for robust dam monitoring in Malaysia, especially involving satellite imagery and various parameters such as rainfall, wind direction and temperature (dry and wet seasons).

5. ACKNOWLEDGMENT

The authors acknowledge the Muda Agricultural Development Authority for providing us with ground-based measurements of water level data. We would also like to thank the Malaysian Space Agency (MYSA) for the opportunity to conduct this research study.

REFERENCES

Al-Husseinawi, Y., Li, Z., Clarke, P., and Edwards, S. 2018. Evaluation of the stability of the Darbandikhan Dam after the 12 November 2017 Mw 7.3 Sarpol-e Zahab (Iran-Iraq Border) Earthquake. *Remote Sens*, 10, pp.1426.

Cohen, J., Cohen, P., West, S.G., and Aiken, L.S., 2013. *Applied multiple regression/correlation analysis for the behavioral sciences.* Routledge.

Cochrance, T.A., Arias, M.E., and Piman, T. 2014. Historical impact of water infrastructure on water levels of the Mekong River and the Tonle Sap system. *Hydrol. Earth Syst. Sci*, 18, pp. 4529–4541.

Gstaiger, V., Huth, J., Gebhardt, S., Wehrmann, T., and Kuenzer, C. 2012. Multi-sensorial and automated derivation of inundated areas using TerraSAR-X and ENVISAT ASAR data. *Int. J. Remote Sens*, 33, pp.7291–7304.

Hong, S.H., Wdowinski, S., Kim, S.W., Won, J.S. 2010. Multi-temporal monitoring of wetland water levels in the Florida Everglades using interferometric Synthetic Aperture Radar (InSAR). *Remote Sens. Environ*, 114, pp. 2436–2447.

Jensen, J. R. 2005. *Introductory Digital Image Processing: A Remote Sensing Perspective*. Prentice Hall, NJ: Pearson,

Lillesand, T.M., Kiefer, R.W. and Chipman, J.W., 2004. *Remote Sensing and Image Interpretation*. 5th Edition, John Wiley & Sons Inc., New York.

Lusch, D. 1999. Introduction to microwave remote sensing, Center for Remote Sensing and Geographic Information Science, Michigan State University: *East Lansing, MI, USA*, pp. 84.

O'Hara, R., Green, S., McCarthy, T. 2019. The agricultural impact of the 2015–2016 floods in Ireland as mapped through Sentinel-1 satellite imagery. *Ir. J. Agric. Food Res*, 58, pp. 44–65.

Sentinel-1 Polarization. Retrieved from https://support.capellaspace.com/hc/en-us/articles/360044738831-Sentinel-1-Polarization.

Shen, X., Wang, D., Mao, K., Anagnostou, E., and Hong, Y. 2019. Inundation extent mapping by Synthetic Aperture Radar: A Review. *Remote Sens*, 11, pp. 879.

Tomás, R., Cano, M., García-Barba, J., Vicente, F., Herrera, G., Lopez-Sanchez, J.M., and Mallorquí, J.J. 2013. Monitoring an earthfill dam using differential SAR interferometry: La Pedrera Dam, Alicante, Spain. *Eng. Geol*, 157, pp. 21–32.

Wdowinski, S., Kim, S.W., Amelung, F., Dixon, T.H., Miralles-Wilhelm, F., Sonenshein, R. 2008. Space-based detection of wetlands' surface water level changes from L-band SAR interferometry. *Remote Sens. Environ*, 112, pp. 681–696.

Yoon, G.W., Kim, S.W., Lee, Y.W., Won, J.S. 2013. Measurement of the water level in reservoirs from TerraSAR-X SAR interferometry and amplitude images. *Remote Sens. Lett*, 4, pp. 446–454.